

# Localization effects in disordered quantum batteries

Mohammad B. Arjmandi<sup>✉\*</sup> and Hamidreza Mohammadi<sup>✉†</sup>  
*Faculty of Physics, University of Isfahan, P.O. Box 81746-7344, Isfahan, Iran. and  
Quantum Optics Research Group, University of Isfahan, Isfahan, Iran*

Andreia Saguia<sup>✉‡</sup> and Marcelo S. Sarandy<sup>✉§</sup>  
*Instituto de Física, Universidade Federal Fluminense, Av. Gal. Milton  
Tavares de Souza s/n, Gragoatá, 24210-346 Niterói, Rio de Janeiro, Brazil*

Alan C. Santos<sup>✉¶</sup>  
*Departamento de Física, Universidade Federal de São Carlos,  
Rodovia Washington Luís, km 235 - SP-310, 13565-905 São Carlos, SP, Brazil*

We investigate the effect of localization on the local charging of quantum batteries (QBs) modeled by disordered spin systems. Two distinct schemes based on the transverse-field random Ising model are considered, with Ising couplings defined on a Chimera graph and on a linear chain with up to next-to-nearest neighbor interactions. By adopting a low-energy demanding charging process driven by local fields only, we obtain that the maximum extractable energy by unitary processes (ergotropy) is highly enhanced in the ergodic phase in comparison with the many-body localization (MBL) scenario. As we turn off the next-to-nearest neighbor interactions in the Ising chain, we have the onset of the Anderson localization phase. We then show that the Anderson phase exhibits a hybrid behavior, interpolating between large and small ergotropy as the disorder strength is increased. We also consider the splitting of total ergotropy into its coherent and incoherent contributions. This incoherent part implies in a residual ergotropy that is fully robust against dephasing, which is a typical process leading to the self-discharging of the battery in a real setup. Our results are experimentally feasible in scalable systems, such as in superconducting integrated circuits.

## I. INTRODUCTION

Few-body devices able to exploit quantum features, such as entanglement and coherence, have been referred to as quantum devices, leading to the second revolution for quantum technologies. They can potentially provide striking advantages, such as more sensitivity [1–4] and high efficient metrology [5–7]. They can also be used for communication tasks [8–11], heat and spin current devices like transistors [12–16] and diodes [17–19], among others [20–26]. Naturally, each of these devices needs energy to operate and this energy, in turn, can be supplied by another quantum storage device, i.e., a quantum battery (QB) [27, 28]. By following the seminal work by Alicki and Fannes [29], QBs are designed as a set of interacting quantum cells, each of them usually represented by a two-level quantum system (qubit). These cells can be charged to store energy (with respect to a reference Hamiltonian) by means of external agents, such as fields, interactions, or any other stimulus able to inject energy into the system. Although QBs are typically composed by qubits, proposals of QB with qutrits [30] and bosonic systems can also be found [31–33].

QBs may exhibit supercharging behavior, with efficiency of energy extraction growing with the number of cells [29]. Such advantage with respect to classical batteries has been at-

tributed to entanglement and quantum correlations [34–41]. However, both constructive and destructive scenarios have been found for the interplay between entanglement and available energy in QBs [34, 42–46]. On the other hand, coherence seems to play an important role for the QB performance [45, 47–52]. As a consensus, collective effects in the dynamics are behind a robust route for designing efficient QBs, when compared with the parallel (non-interacting) charging of the system [53]. From the experimental point of view, the energy storing properties of a diversity of quantum systems have been exploited, with physical realizations in a number of architectures, such as nuclear magnetic resonance [54], superconducting integrated circuits [55, 56], metal complex [57], and an all-optical setup [58].

Here, we aim at investigating quantum phases of matter that may be suitable for qubit-based QBs. Concretely, we will focus on the ergotropy and charging power of quantum devices subject to disordered couplings and external fields. As sketched in Fig. 1, two distinct schemes for QBs based on the transverse-field random Ising model will be considered, with Ising couplings defined on a Chimera graph (for a physical realization, see e.g. Ref. [59]) and on a linear chain with up to next-to-nearest neighbor interactions [60]. Analyses of disorder effects in the performance of QBs have been previously considered in the literature, such as in Refs. [61, 62]. However, differently from previous works, where time-dependent interactions drive the charging process, we adopt permanent interactions, so that the QB charging is performed through external local fields only. Our approach is motivated by the fact that switching on/off interactions typically costs a significant amount of energy in comparison with the ergotropy provided by the QB [57]. As a result, we obtain that the ergodic phase

\* m.arjmandi@sci.ui.ac.ir

† hr.mohammadi@sci.ui.ac.ir

‡ asaguia@id.uff.br

§ msarandy@id.uff.br

¶ ac.santos@df.ufscar.br

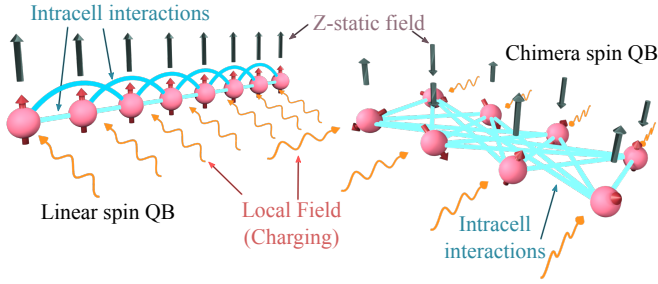


Figure 1. Two distinct schemes of QBs based on the transverse-field random Ising model are considered: (i) Ising couplings on a linear chain with up to next-to-nearest neighbor interactions (left) and (ii) Ising couplings defined on a Chimera graph (right). For both models, the charging process is locally driven by an external field. The set of intracell interactions defines the kind of model adopted, such that different phases can be obtained as a function of the disorder strength.

favors the QB performance, with disorder being detrimental to ergotropy due to the memory effects in the many-body localization (MBL) phase. Remarkably, when Anderson localization is available, we have a hybrid scenario between ergodic and MBL behaviors depending on the disorder strength. We also address the splitting of ergotropy into coherent and incoherent contributions, showing that a residual extractable work robust against dephasing can be stored as incoherent ergotropy [51].

## II. PRELIMINARIES

We review now the concept of ergotropy and introduce the quantum spin systems adopted as models of QB in our work.

### A. Ergotropy

The energy available to be extracted in the form of work in a QB depends on both the state  $\rho$  of the quantum device and the reference Hamiltonian  $H_{\text{ref}}$  that sets the energy scale of the system. Given  $\rho$  and  $H_{\text{ref}}$ , the internal energy is provided by the expectation value  $E(\rho, H_{\text{ref}}) = \text{tr}(\rho H_{\text{ref}})$ . By keeping a constant entropy, work can be performed by/on the QB by unitary operations. In this scenario, we define *ergotropy* as the maximum energy extractable by realizing unitary operations on the system [63]. Therefore, ergotropy reads

$$\mathcal{E}(\rho, H_{\text{ref}}) = \max_U \left[ E(\rho, H_{\text{ref}}) - E(U\rho U^\dagger, H_{\text{ref}}) \right]. \quad (1)$$

The maximization over  $U$  is achieved by driving the QB towards the *passive state*  $\bar{\rho} \equiv U\rho U^\dagger$  associated with  $\rho$ , i.e., a state that cannot provide further energy by unitary operations. We can compute  $\mathcal{E}(\rho, H_{\text{ref}})$  by looking at the spectral decompositions of  $\rho = \sum_{i=1}^d p_i |p_i\rangle\langle p_i|$  and  $H_{\text{ref}} = \sum_{i=1}^d \epsilon_i |\epsilon_i\rangle\langle \epsilon_i|$ , where we assume the ordering  $p_1 \geq p_2 \geq \dots \geq p_d$  and  $\epsilon_1 \leq \epsilon_2 \leq \dots \leq \epsilon_d$ , with  $d$  being the dimension of the Hilbert space. Thus, ergotropy can be rewritten as [63] (see also

Refs [64, 65])

$$\mathcal{E}(\rho, H_{\text{ref}}) = E(\rho, H_{\text{ref}}) - \sum_{i=1}^d \epsilon_i p_i. \quad (2)$$

Notice that both the internal energy and the ergotropy depend on the reference Hamiltonian  $H_{\text{ref}}$ . In the charging process of a QB, we also add a charging Hamiltonian  $H_{\text{ch}}(t)$ , yielding a total driving Hamiltonian  $H_d(t) = H_{\text{ref}} + H_{\text{ch}}(t)$ . Let us take  $H_{\text{ref}} = H_0 + H_{\text{int}}$ , where  $H_0$  is a local Hamiltonian and  $H_{\text{int}}$  contains the native system interactions. Then, any additional cost to charge the battery comes from the charging Hamiltonian  $H_{\text{ch}}(t)$ . More precisely, the cost to turn-on and turn-off the term  $H_{\text{ch}}(t)$  should be considered in the energy balance of the device, which may lead to non-efficient quantum batteries [57]. Here, to avoid the cost of engineering non-native interactions, we focus on a charging process driven only by external local fields.

### B. QB Models

As sketched in Fig. 1, we consider two distinct models of QB, with many-body localization regimes properly characterized. First, let us consider an  $N$ -particle random spin-1/2 Ising linear chain with on-site magnetic static field  $h_k$ . The native interactions are provided by nearest neighbor ( $J_k^{(1)}$ ) and next-to-nearest neighbor ( $J_k^{(2)}$ ) couplings. The reference Hamiltonian of the system reads

$$H_{\text{ref}}^{\text{Isi}} = \sum_{k=1}^N h_k \sigma_k^z - \sum_{k=1}^{N-1} J_k^{(1)} \sigma_k^x \sigma_{k+1}^x + \sum_{k=1}^{N-2} J_k^{(2)} \sigma_k^x \sigma_{k+2}^x, \quad (3)$$

where  $\sigma^\alpha$  ( $\alpha = x, y, z$ ) are the standard Pauli matrices. The QB is charged according to a transverse local field through a charging Hamiltonian

$$H_{\text{ch}} = \sum_k^N \Omega_k \sigma_k^x. \quad (4)$$

This driving field can be implemented, for instance, through an oscillating small radio-frequency magnetic field of intensity  $|B_{\text{rf}}| \propto \Omega_k$ , as in a nuclear magnetic resonance setup [66]. We assume local fields uniformly distributed over the chain, with  $h_k = h$  and  $\Omega_k = \Omega$  constant couplings. In this model, the random nature of the system relies on the interactions between nearest neighbors given by  $J_k^{(1)}$ , as selected from a uniform distribution in the interval  $[J_0(1 - \delta), J_0(1 + \delta)]$ , where  $J_0$  sets the energy scale of the system and  $\delta$  is a dimensionless parameter that determines the degree of disorder. Concerning the next-to-nearest neighbor coupling  $J_k^{(2)}$ , it will also be taken as a constant chosen as a function of  $J_0$ . For the charging process we assume  $J_0 = \Omega$ .

The localization properties of random spin-1/2 Ising chains have been widely studied [60]. In particular, as the next-to-nearest neighbor interaction is turned off ( $J_k^{(2)} = 0$ ), the model reduces to the well known nearest neighbor transverse field

Ising chain, such that an arbitrary amount of disorder ( $\delta > 0$ ) brings the system into an Anderson localization regime [67]. However, when  $J_k^{(2)} \neq 0$ , the degree of disorder needs to be strong enough to drive the system to many-body localization (MBL), otherwise the system remains in an ergodic phase [67–69]. Unless specified otherwise, we refer to the various phases of this model by adopting the specific values for the couplings: (i) Anderson localized:  $J_k^{(2)} = 0$  and  $\delta = 1$ ; (ii) Ergodic phase:  $J_k^{(2)} = h/2 = 0.3J_0$  and  $\delta = 1$ , and (iii) MBL phase:  $J_k^{(2)} = h/2 = 0.3J_0$  and  $\delta = 5$ .

It is worth mentioning that this model was previously considered to investigate localization effects on QB [62]. However, in Ref. [62], the authors assume the QB is charged through *turned-on* interactions between the quantum cells of the battery during charging time. Then, all figures of merit are evaluated with respect to the free part of the Hamiltonian, i.e., the on-site applied field. As previously mentioned, the energy cost of switching on/off the interactions might be detrimental to the performance of the QB, with the energy cost to charge the battery much larger than the ergotropy itself [57, 70]. Here, we analyze the energy cost of the charging process in Appendix A, showing that the charging through a local field only is an energy friendly choice.

As our second QB model, we consider random Ising interactions and local fields defined on the 8-spin Chimera unit cell, as sketched in Fig. 1. The reference Hamiltonian reads

$$H_{\text{ref}}^{\text{Chi}} = \sum_k h_k \sigma_k^z + \sum_{\langle k, j \rangle \in C_{\text{Chi}}} J_{kj} \sigma_k^z \sigma_j^z, \quad (5)$$

where the  $\langle k, j \rangle \in C_{\text{Chi}}$  refers to a sum over the connections of the Chimera graph. Concerning the charging Hamiltonian  $H_{\text{ch}}$ , it will be defined through transverse local fields, as in Eq. (4), with constant couplings  $\Omega_k = \Omega$ . For this system, we consider random values for both  $h_k$  and  $J_{kj}$  from a uniform distribution  $[-\delta J_0, \delta J_0]$ , with  $\delta$  being the disorder amplitude, such that  $\delta J_0$  is the maximum admissible value for the coupling strength. Taking into account the characterization of the MBL phase transition as in Ref. [59], with  $J_0 = \Omega$ , we will adopt the specific values for the disorder strength: (i) Ergodic phase:  $\delta = 2$ , such that  $\delta J_0 = 2\Omega$  and (ii) MBL phase:  $\delta = 6$ , such that  $\delta J_0 = 6\Omega$ . It is worth mentioning that, while the Anderson localized phase is well defined for the random Ising chain in the absence of next-to-nearest-neighbor interactions (i.e., when  $J_2 = 0$ ) [71], we do not expect that the chimera topology will exhibit Anderson localization for the regime of couplings considered here.

By disregarding decoherence effects, the dynamics of the QB is governed by the unitary evolution operator  $U(t)$  as  $\rho(t) = U(t)\rho(0)U^\dagger(t)$ . We assume the device starts from its fully empty state  $\rho(0) = |G\rangle\langle G|$ , where  $|G\rangle$  is the ground state of the reference Hamiltonian for each model (empty energy state of the battery). Given the randomness of local fields and interaction strengths, we will have a distinct reference Hamiltonian  $H_{n,\text{ref}}$  for each disorder realization. Therefore, it is expected that the ergotropy will change for different choices of the random parameters. For this reason, to define a fair figure of merit to evaluate the QB performance, we will consider the

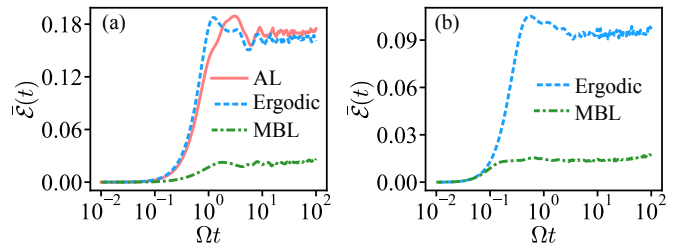


Figure 2. The dynamics of average ergotropy for (a) the  $N = 8$  random Ising chain with next-to-nearest neighbors and (b) the random Ising model on the 8-spin Chimera graph. The number of realizations is taken as  $N_r = 100$ . The Hamiltonian parameters for each phase are set as described in Sec. II B.

average ergotropy over  $N_r$  realizations of disorder [65]

$$\bar{\mathcal{E}}(t) = \frac{1}{N_r} \sum_{n=1}^{N_r} \frac{\mathcal{E}(\rho_n(t), H_{n,\text{ref}})}{\mathcal{E}_n^{\text{max}}}, \quad (6)$$

where  $\mathcal{E}(\rho_n(t), H_{n,\text{ref}})$  is the time-dependent ergotropy associated with the evolved state  $\rho_n(t)$  for the  $n$ -th realization. We also define  $\mathcal{E}_n^{\text{max}} = \text{tr}(\rho_{n,\text{fc}} H_{n,\text{ref}}) - \text{tr}(\rho_{n,G} H_{n,\text{ref}})$  as the maximum capability of the battery, i.e., the ergotropy stored in its fully charged state  $\rho_{n,\text{fc}}$ , with  $\rho_{n,G}$  denoting the density operator for the ground state of  $H_{n,\text{ref}}$ . Because we assume pure states (unitary evolution),  $\rho_{n,\text{fc}}$  is the eigenstate of  $H_{n,\text{ref}}$  with the highest eigenvalue [63, 72]. In this way, we can measure the charge in the QB with the reference Hamiltonian  $H_{n,\text{ref}}$  for a given realization  $n$ , with respect to the maximally charged state  $\rho_{n,\text{fc}}$ . Throughout this work we show the results for the case with  $N_r = 100$ , but it is worth saying that we do not observe any significant change by taking  $N_r > 100$ .

### III. RESULTS AND DISCUSSION

#### A. Ergotropy and charging power

Now, we present our main results. First of all, we evaluate the ergotropy by charging the battery in the different phases aforementioned. In Fig. 2, we show the dynamics of the average ergotropy for both models considered in our work, where we conclude that the MBL phase turns out to be a poor choice for a QB in the sense of energy storage. This can be explained by the emergence of memory effects attributed to the MBL phase with respect to the initial state [59, 73], which in turn prevents the QB from a significant evolution with respect to its ground state. If the dynamics starts from a different state, an enhancement of the charging performance is expected, but it requires the initialization step by using a different reference Hamiltonian. For example, in Ref. [62], the authors considered the initial state as the lowest energy level of the non-interacting quantum cells, which will demand an extra cost as we turn on the interactions throughout the charging process.

Differently from the MBL phase, where the “frozen” dynamics handicaps the energy charging, the battery presents a charging enhancement in either the ergodic or Anderson

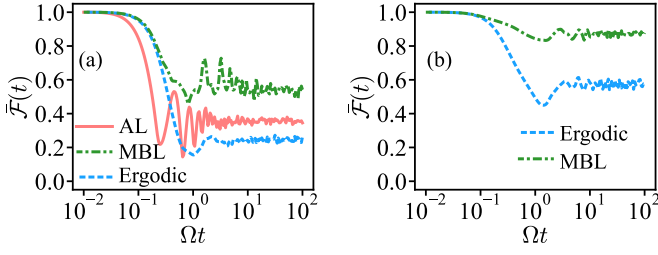


Figure 3. Average fidelity  $\bar{\mathcal{F}}(t)$  as defined by Eq. (7) for (a) the  $N = 8$  random Ising chain with next-to-nearest neighbors and (b) the random Ising model on the 8-spin Chimera graph. The number of realizations is taken as  $N_r = 100$ . The Hamiltonian parameters for each phase are set as described in Sec. II B.

phases. In the case of the ergodic phase, such a result can be explained by its delocalization behavior, which makes the ergodic phase more suitable for ergotropy deposition. Notice that the Anderson phase follows a similar pattern as obtained in the ergodic phase for the chosen disorder strength, also showing a remarkable difference with respect to the MBL phase in terms of ergotropy. Due to the absence of strong memory effects typical of the MBL phase, the dynamics of QB in the Anderson phase is not frozen so that it shows a suitable performance. Moreover, for a wide time interval, which is around the range  $[10^0, 10^2]$ , the Anderson phase presents a performance even better than the ergodic case. We can reach a more precise view at the above discussion by analyzing the memory effects of MBL phase and its poor performance for ergotropy storage. To this end, we need to know how the evolved state of the QB looks like when compared to its initial ground state. More resemblance to the initial state can be inferred as a sign of retaining information about the past and, consequently, indicating a memory effect. Therefore, we consider the average fidelity, taken over  $N_r$  disorder realizations, between the time-dependent density operator of the QB and its initial ground state, which reads

$$\bar{\mathcal{F}}(t) = \frac{1}{N_r} \sum_{n=1}^{N_r} \mathcal{F}(\rho_n(t), \rho_{n,G}), \quad (7)$$

where the fidelity of two general density matrices  $\rho$  and  $\sigma$  is defined by  $\mathcal{F}(\rho, \sigma) = \text{Tr} \sqrt{\sqrt{\rho}\sigma\sqrt{\rho}}$ . As shown in Fig. 3 the highest fidelity over the considered charging time belongs to the MBL phase, implying the minimum change in the state of the QB with respect to its initial preparation. This fact is more visible for the Chimera model. Let us now analyze the time-averaged charging power of the QB as a function of time. Notice that, as shown in from Fig. 2, the maximum instantaneous amount of ergotropy is achieved for different instants of time for each phase considered. Then, it is meaningful to consider the time-averaged charging power in the parametrized time interval  $\Omega\Delta t = \Omega(t - t_0)$  (assuming here  $t_0 = 0$ ). In this context, by using the notation introduced in Eq. (6), we can introduce the dimensionless power parameter

$$\bar{P}_0(\Delta t) = \frac{\bar{\mathcal{E}}(t) - \bar{\mathcal{E}}(0)}{\Omega\Delta t}. \quad (8)$$

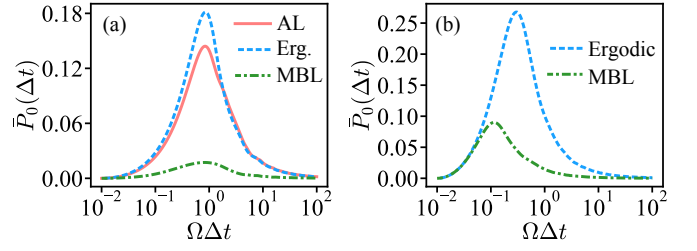


Figure 4. The dynamics of averaged charging power for (a) the  $N = 8$  random Ising chain with next-to-nearest neighbors and (b) the random Ising model on the 8-spin Chimera graph. The number of realizations is taken as  $N_r = 100$ . The Hamiltonian parameters for each phase are set as described in Sec. II B.

Notice that  $\bar{P}_0(\Delta t)$  is directly related to the average power  $P(\Delta t)$ . Indeed,  $P(\Delta t)$  can be written in terms of the average of the maximum ergotropy capability of the battery  $\bar{\mathcal{E}}^{\max} = \sum_{n=1}^{N_r} \mathcal{E}_n^{\max}/N_r$ , the charging field amplitude  $\Omega$ , and the parameter  $\bar{P}_0(\Delta t)$  as  $P(\Delta t) = \Omega\bar{\mathcal{E}}^{\max}\bar{P}_0(\Delta t)$ . Through the above definition, we can collect information about the charging performance (including the optimal charging time window  $\Delta t_{\text{opt}}$ ) defined over the entire time-domain of the charging process, which makes this analysis more robust than simply finding the optimal charging time for the battery. For both models, as it can be seen from Fig. 4, the QB in the ergodic phase is more powerful than the other phases for the range of time considered. Then, while the Anderson phase may allow for storing more energy than the ergodic phase for a specific time range, its charging power is not as efficient as the ergodic QB.

For completeness of our discussions, it is worth mentioning that different behaviors for the ergotropy and phase-dependent battery performance can be drastically modified for other kinds of fields chosen to charge the battery. We identified that such a change is mainly due to the charging-field induced change in the localization transition of the system, then leading to a significant effect on the nature of the models and their quantum phases (for more details, see Appendix B.) In addition, in Appendix C we included a brief analysis of the expected negative effects of random next-to-nearest neighbor interaction ( $J_2$ ). As a conclusion of this case, we observe that a small reduction in the quality of charging process is expected when introducing this extra randomness, such that additional efforts to engineer random next-to-nearest neighbor couplings  $J_2$  do not help the charging process.

So far, our results suggest that the disorder strength seems to be the main determinant for ergotropy and power rather than the quantum (ergodic or Anderson) phase the system actually is. In fact, the charging of the QB in the Anderson localized and ergodic phases are performed by using an equal degree of disorder ( $\delta = 1$ ), while the MBL phase requires stronger disorder. The role played by disorder can be confirmed by considering the Anderson phase for different degrees of randomness. This is shown in Fig. 5, where we have plotted ergotropy and dimensionless power in the Anderson phase for the Ising linear chain for different values of  $\delta$ . Notice that the Anderson phase then interpolates between the ergodic and MBL behaviors as we increase the strength of disorder.

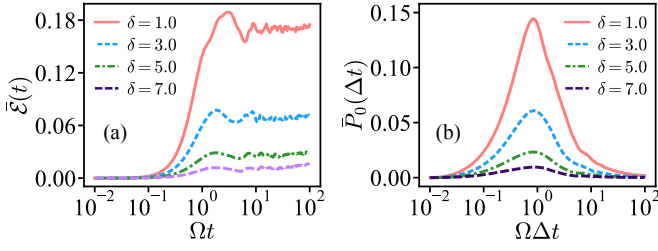


Figure 5. The dynamics of (a) average ergotropy and (b) power for the  $N = 8$  random Ising chain in the Anderson phase for different degrees of disorders. The number of realizations is taken as  $N_r = 100$ . The Hamiltonian parameters for each phase are set as described in Sec. II B.

### B. Incoherent and coherent ergotropy

Let us now split ergotropy into its *coherent* and *incoherent* contributions [51]. The generation of quantum superpositions (coherence) in the energy basis during the charging leads to a non-zero amount of coherent ergotropy. On the other hand, part of the total ergotropy is stored as incoherent ergotropy. In particular, the incoherent part of the ergotropy is relevant in our discussion because it takes into account the “residual” ergotropy of the *dephased* state  $\rho^D$  in energy eigenbasis of the reference Hamiltonian, with  $\rho^D = \sum_i^d \langle \epsilon_i | \rho | \epsilon_i \rangle | \epsilon_i \rangle \langle \epsilon_i |$ . Physically speaking, it quantifies the total amount of ergotropy that remains in the system, even in absence of an external charging field under a dephasing process. Therefore, we can identify this amount of remaining ergotropy as related to the robustness of a QB against its *self-discharging process* [49].

Inspired by Ref. [51], we introduce the average normalized incoherent and coherent ergotropy, respectively, as

$$\bar{\mathcal{E}}_{\text{Inco}}(t) = \frac{1}{N_r} \sum_{n=1}^{N_r} \frac{\mathcal{E}(\rho_n^D(t), H_{n,\text{ref}})}{\mathcal{E}_n^{\text{max}}}, \quad (9)$$

$$\bar{\mathcal{E}}_{\text{Cohe}}(t) = \frac{1}{N_r} \sum_{n=1}^{N_r} \frac{\mathcal{E}(\rho_n(t), H_{n,\text{ref}}) - \mathcal{E}(\rho_n^D(t), H_{n,\text{ref}})}{\mathcal{E}_n^{\text{max}}}. \quad (10)$$

Fig. 6 shows the time evolution of  $\bar{\mathcal{E}}_{\text{Inco}}(t)$  and  $\bar{\mathcal{E}}_{\text{Cohe}}(t)$  for different phases of the models considered in our work. Given the good qualitative agreement between the behavior of the total extractable energy and its coherent and incoherent parts, we can safely state that the performance of the QB is mainly related to the coherence generated during its charging, since the extractable work is mainly stored as coherent ergotropy. However, by comparing Fig. 2 and Fig. 6, it can be inferred that, even though the total ergotropy is mostly consisted of coherent part, there remains a nonzero amount of incoherent ergotropy during charging process. This can be useful in a real setup since, as discussed above, the incoherent ergotropy is robust against dephasing channels, since its corresponding state is already dephased in the basis of eigenenergies. It is worth mentioning that the incoherent ergotropy can be wasted under dissipation processes through population relaxation. Nonetheless, one may find a situation in which pure dephasing is the main dominant process, namely for quantum dots [74–77] or

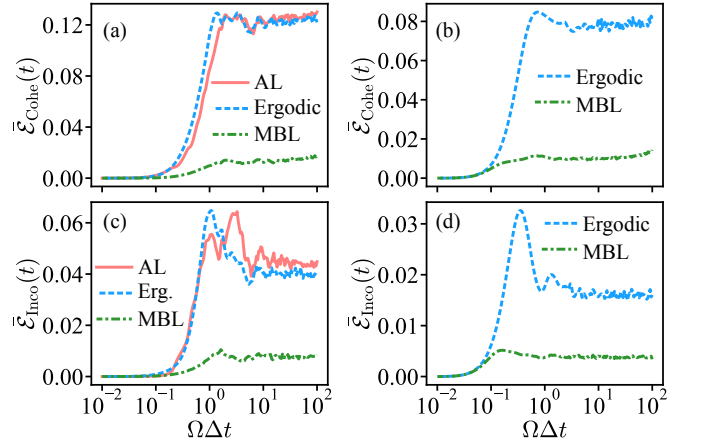


Figure 6. The dynamics of coherent and incoherent ergotropy for (a), (c) the  $N = 8$  random Ising chain with next-to-nearest neighbors and (b), (d) the random Ising model on the 8-spin Chimera graph. The number of realizations is taken as  $N_r = 100$ . The Hamiltonian parameters for each phase are set as described in Sec. II B.

trapped ions [78, 79], resulting in potential usefulness of the incoherent ergotropy.

We can now analyze the average normalized coherence  $\overline{QC}(t)$  generated for each dynamics as quantified by the  $l_1$ -norm, which is defined as

$$\overline{QC}(t) = \frac{1}{N_r} \sum_{n=1}^{N_r} \left[ \frac{1}{C_{\text{max}}} \sum_{i,j \neq i} |\rho_{ij}| \right], \quad (11)$$

In Eq. (11), the term in “brackets” is the  $l_1$ -norm coherence of the density matrix for each realization  $n$ , where  $C_{\text{max}}$  denotes the coherence of the quantum state  $(|e\rangle + |g\rangle) / \sqrt{2}$ , which is the maximally coherent state in the local basis  $\{|e\rangle, |g\rangle\}$ . The results for  $\overline{QC}(t)$  are shown in Fig. 7 for both the Ising chain and the Chimera graph. Comparing Figs. 2b and 7b, for the Chimera graph, quantum coherence can be regarded as a suitable figure of merit of the stored ergotropy, at least qualitatively. As time passes by, both quantities sharply increase when the QB is in the ergodic phase but they are small for the MBL phase. This is not the case for the Ising chain. The model contains some amount of initial quantum coherence but localized phases reach more coherence in comparison with the ergodic phase. The relation between generation of ergotropy and coherence is then model-dependent, i.e., different patterns of interactions may imply in different qualitative relations.

## IV. CONCLUSIONS

We have investigated quantum phases of disordered spin systems as a model of qubit-based QBs. Differently from previous investigations, we have focused on the local ergotropy injection through external fields only. This is due to the low energy demanding property of this scheme in comparison with the time-dependent switchable interacting systems. For the models considered in our work, ergodicity has shown to improve the QB performance, with disorder being detrimental to

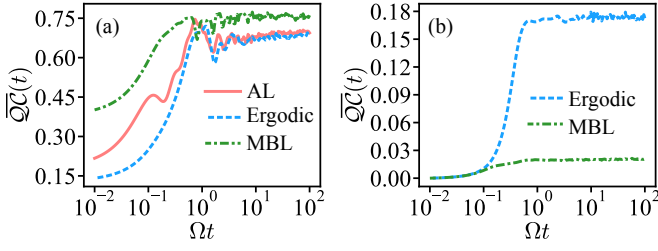


Figure 7. Average quantum coherence for (a) the  $N = 8$  random Ising chain with next-to-nearest neighbors and (b) the random Ising model on the 8-spin Chimera graph. The number of realizations is taken as  $N_r = 100$ . The Hamiltonian parameters for each phase are set as described in Sec. II B.

ergotropy due to the memory effects of the discharged state in the MBL phase. In the case of the linear Ising chain, where Anderson localization is induced for any amount of disorder as the next-to-nearest interaction is turned off, we have shown the presence of a hybrid scenario interpolating between ergodic and MBL behaviors depending on the disorder strength. It is worth highlighting here that, while the MBL phase is attractive for time-dependent interacting QBs [62], it develops a poor performance for the local charging scheme. Concerning quantum coherence, we identified that most of ergotropy is stored as coherent ergotropy, which provides the quantum character of the energy storing device. On the other hand, we also obtained a nonvanishing amount of incoherent ergotropy, which indicates robustness of the storage capability against the self-discharging of QBs due to dephasing (see, e.g., Refs. [49] and [51]). Further investigations of lattice topologies and quantum phases in disordered systems as well as experimental implementations are left for a future analysis.

## ACKNOWLEDGMENTS

M.S.S. is supported by Conselho Nacional de Desenvolvimento Científico e Tecnológico (CNPq) (307854/2020-5). A.C.S. acknowledges the financial support of the São Paulo Research Foundation (FAPESP) (Grant No. 2019/22685-1). This research is also supported in part by Coordenação de Aperfeiçoamento de Pessoal de Nível Superior (CAPES) (Finance Code 001) and by the Brazilian National Institute for Science and Technology of Quantum Information (INCT-IQ).

### Appendix A: Energy cost of switching on/off interactions

In this section, we analyze the energy cost of turning on/off the intracell interactions for both models of QB considered in our work. For the spin-1/2 Ising chain with nearest and next-to-nearest neighbor interactions we have  $H_{\text{ref}}^{\text{Isi}} = H_0^{\text{Isi}} + H_{\text{int}}^{\text{Isi}}$ , where

$$H_0^{\text{Isi}} = h \sum_{k=1}^N \sigma_k^z, \quad H_{\text{int}}^{\text{Isi}} = - \sum_{k=1}^{N-1} J_k \sigma_k^x \sigma_{k+1}^x + J_2 \sum_{k=1}^{N-2} \sigma_k^x \sigma_{k+2}^x. \quad (\text{A1})$$

For the Ising couplings defined on the Chimera graph, we also have  $H_{\text{ref}}^{\text{Chi}} = H_0^{\text{Chi}} + H_{\text{int}}^{\text{Chi}}$  where

$$H_0^{\text{Chi}} = \sum_k h_k \sigma_k^z, \quad H_{\text{int}}^{\text{Chi}} = \sum_{k,j} J_{kj} \sigma_k^z \sigma_j^z. \quad (\text{A2})$$

We introduce the energy cost  $C_{\text{int}}$  to implement the interactions as the difference between the norm of the reference Hamiltonian including interactions ( $H_{\text{ref}}$ ) and the norm of the reference Hamiltonian without interactions ( $H_0$ ). Mathematically, we have

$$C_{\text{int}} = \mathcal{N}(H_{\text{ref}}) - \mathcal{N}(H_0), \quad (\text{A3})$$

where  $\mathcal{N}(A) = \sqrt{\text{Tr}(A^\dagger A)}$  is the Hilbert-Schmidt norm of a given (finite-dimensional) matrix  $A$ . Our definition based on the Hilbert-Schmidt norm is motivated by previous works showing that such a quantity is a good measure of energy cost for quantum control in different contexts [80–83], including experiments [84, 85]. More precisely, it is related to a measure of the thermodynamic cost of an arbitrary unitary quantum evolution [86]. In this way, one can show that, for the Ising chain, the cost reads

$$C_{\text{int}}^{\text{Isi}} = 16 \left( -2\sqrt{4h^2} + \sqrt{8h^2 + 6J_2^2 + \sum_k J_k^2} \right), \quad (\text{A4})$$

while, for the Chimera graph, we have

$$C_{\text{int}}^{\text{Chi}} = 16 \left( -\sqrt{\sum_k h_k^2} + \sqrt{\sum_k h_k^2 + \sum_{k,j} J_{kj}^2} \right). \quad (\text{A5})$$

In our work, interactions are always present and we only turn-on and turn-off the charging field. Then, we define the energy cost  $C_{\text{ch}}$  of charging with local chargers as the difference between the norm of the driving Hamiltonian (including reference Hamiltonian and any local charging fields) and the norm of the reference Hamiltonian. Mathematically, we write

$$C_{\text{ch}} = \mathcal{N}(H) - \mathcal{N}(H_{\text{ref}}), \quad (\text{A6})$$

where  $H = H_{\text{ref}} + H_{\text{ch}}$  is the total driving Hamiltonian. Again, one can simply obtain the explicit form of this cost for the two models

$$C_{\text{ch}}^{\text{Isi}} = 16 \left( \sqrt{\Xi^2 + 8\Omega^2} - |\Xi| \right), \quad (\text{A7})$$

$$C_{\text{ch}}^{\text{Chi}} = 16 \left( \sqrt{\Lambda^2 + 8\Omega^2} - |\Lambda| \right). \quad (\text{A8})$$

with  $\Xi^2 = 8h^2 + 6J_2^2 + \sum_k J_k^2$ , and  $\Lambda^2 = \sum_k h_k^2 + \sum_{k,j} J_{kj}^2$ .

To compute the energy cost we define here the quantity

$$\bar{C}_{\text{ch}} = \frac{1}{N_r} \sum_{n=1}^{N_r} \frac{C_{\text{ch},n}}{\mathcal{E}_n^{\text{max}}}, \quad (\text{A9})$$

where  $C_{\text{ch},n}$  denotes the charging cost for each model, as given by Eqs. (A4), (A5), (A7) and (A8), in the  $n$ -th realization. It quantifies the average normalized energy cost of the charging

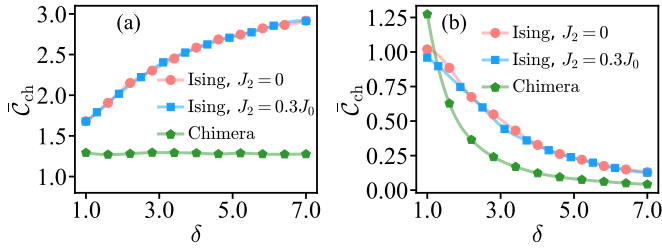


Figure 8. Cost of turning on/off (a) intracell interactions, and (b) local charging fields as function of the degree of disorder for the  $N = 8$  random Ising chain with next-to-nearest neighbors and the random Ising model on the 8-spin Chimera graph. The number of realizations is taken as  $N_r = 100$ . The Hamiltonian parameters for each phase are set as described in Sec. II B.

(either with interactions or local fields) as a multiple of the maximum capability  $\mathcal{E}_n^{\text{max}}$  of the QB for each model. We apply this definition to all models considered in this work in order to compare the energy cost for charging by using time-dependent intracell interactions and the cost for the case where we charge the battery by using local fields. In Fig. 8 we present the cost for each model as function of the degree of disorder. For all models considered here as energy storing quantum devices, the charging by local fields is energetically more efficient than the time-dependent interaction engineering, particularly when disorder is strong enough. In particular, the advantage of the local charging comes from the fact that, for high disorder, the interaction dominates over the local charging field as  $\mathcal{N}(H) \rightarrow \mathcal{N}(H_{\text{ref}})$ , providing  $C_{\text{ch},n} \ll \mathcal{E}_n^{\text{max}}$  for each model. We stress that while this limit is consistent, it does not imply that we have zero cost to implement the charging.

### Appendix B: Oscillating charging fields

Let us consider now a charging protocol given by an oscillating classical field acting locally on each quantum cell of the battery. The corresponding charging Hamiltonian is given by

$$H_{\text{ch}} = \sum_k^N \Omega_k \cos(\omega_k^p t) \sigma_k^x, \quad (\text{B1})$$

where  $\Omega_k = \Omega$  and  $\omega_k^p$  denote the amplitude of the periodic charging field and its frequency applied to the  $k$ -th cell, respectively. First of all, notice that, for such a field, the condition  $\delta = 6$ , such that  $\delta J_0 = 6\Omega$ , for the MBL phase of the Chimera graph is broken down. Indeed, notice that we have now the change  $\Omega \rightarrow \Omega(t) = \Omega \cos(\omega_k^p t)$ . Then,  $\delta J_0 = 6\Omega$  is only satisfied as  $\omega_k^p t = 2n\pi$  ( $n \in \mathbb{Z}$ ). Therefore, the localization pattern may be affected by the choice of the charging Hamiltonian. By modifying the charging term, we may significantly affect the nature of the models and their quantum phases.

Now for completeness, let us discuss the battery performance by keeping the phase pattern while slightly replacing Eq. (4) for a periodic charging Hamiltonian in Eq. (B1). For simplicity, we set them to be identical for each cell, i.e.,  $\omega_k^p = \omega^p$ . By taking this selection of charging fields, we plot the average ergotropy of the QB [by making use of Eq. (6)]. This is shown in Fig. 9, where it can be seen that we have the same charging pattern as before. Once again, we see that ergotropy storage is small in the MBL phase. Moreover, for the Ising chain, there is a similar behavior for ergodic and AL phases (again with slightly better performance in favor of the AL phase).

### Appendix C: Next-to-nearest neighbor disorder effects

In this section, we address the effect of disorder in the next-to-nearest neighbor (NNN) interaction terms. To tackle this point, we randomize the NNN coupling strength, such that  $J_2$  is randomly selected from the uniform distribution  $[-\delta, \delta]$ . The disorder strength  $\delta$  is set to be the same as for the nearest-neighbor interactions. First of all, we remark that in this scenario  $J_2 \neq 0$  leads to absence of Anderson localized phase in the Ising model, so here we exclude this phase from our analysis. In Fig. 9c, we compare the average ergotropy of the Ising model in its various phases along with the curves for the ergodic and MBL phases with random NNN interactions. As a main result of this analysis, we observe that this extra randomness reduces the quality of the charging process, since the overall amount of ergotropy is decreased compared to the previous cases where  $J_2$  is fixed.

- 
- [1] C. L. Degen, F. Reinhard, and P. Cappellaro, Quantum sensing, *Reviews of modern physics* **89**, 035002 (2017).
- [2] Z. Zhang and Q. Zhuang, Distributed quantum sensing, *Quantum Science and Technology* **6**, 043001 (2021).
- [3] S. E. Crawford, R. A. Shugayev, H. P. Paudel, P. Lu, M. Syam Lal, P. R. Ohodnicki, B. Chorpeneing, R. Gentry, and Y. Duan, Quantum sensing for energy applications: Review and perspective, *Advanced Quantum Technologies* **4**, 2100049 (2021).
- [4] D. Feng, Review of quantum navigation, in *IOP Conference Series: Earth and Environmental Science*, Vol. 237 (IOP Publishing, 2019) p. 032027.
- [5] K. Poulsen, A. C. Santos, and N. T. Zinner, Quantum wheatstone bridge, *Phys. Rev. Lett.* **128**, 240401 (2022).
- [6] V. Giovannetti, S. Lloyd, and L. Maccone, Advances in quantum metrology, *Nature photonics* **5**, 222 (2011).
- [7] V. Giovannetti, S. Lloyd, and L. Maccone, Quantum metrology, *Phys. Rev. Lett.* **96**, 010401 (2006).
- [8] C. H. Bennett, G. Brassard, C. Crépeau, R. Jozsa, A. Peres, and W. K. Wootters, Teleporting an unknown quantum state via dual classical and einstein-podolsky-rosen channels, *Phys. Rev. Lett.* **70**, 1895 (1993).
- [9] J. Yin, J.-G. Ren, H. Lu, Y. Cao, H.-L. Yong, Y.-P. Wu, C. Liu, S.-K. Liao, F. Zhou, Y. Jiang, *et al.*, Quantum teleportation and

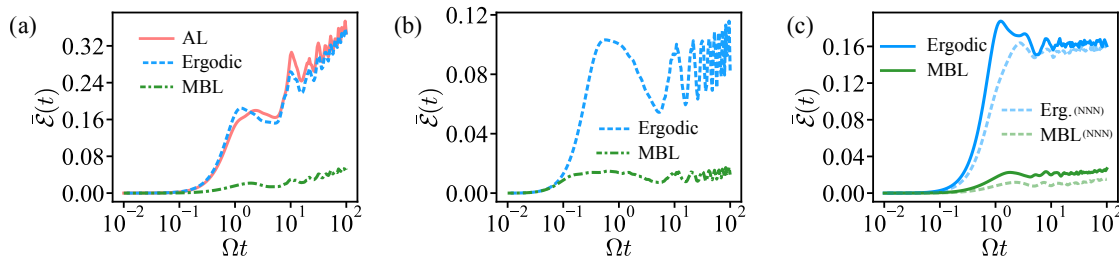


Figure 9. (a,b) The dynamics of average ergotropy with periodic charging field for (a) Ising chain (b) Chimera graph. The number of realizations is taken as  $N_r = 100$ ,  $\Omega = J_0$  and  $\omega^p = 0.3J_0$ . (c) The dynamics of average ergotropy for the various phases of the Ising model compared to the new results with random NNN interactions. We adopt the same parameters as in Fig. 2.

entanglement distribution over 100-kilometre free-space channels, *Nature* **488**, 185 (2012).

- [10] X.-S. Ma, T. Herbst, T. Scheidl, D. Wang, S. Kropatschek, W. Naylor, B. Wittmann, A. Mech, J. Kofler, E. Anisimova, *et al.*, Quantum teleportation over 143 kilometres using active feed-forward, *Nature* **489**, 269 (2012).
- [11] J.-G. Ren, P. Xu, H.-L. Yong, L. Zhang, S.-K. Liao, J. Yin, W.-Y. Liu, W.-Q. Cai, M. Yang, L. Li, K.-X. Yang, X. Han, Y.-Q. Yao, J. Li, H.-Y. Wu, S. Wan, L. Liu, D.-Q. Liu, Y.-W. Kuang, Z.-P. He, P. Shang, C. Guo, R.-H. Zheng, K. Tian, Z.-C. Zhu, N.-L. Liu, C.-Y. Lu, R. Shu, Y.-A. Chen, C.-Z. Peng, J.-Y. Wang, and J.-W. Pan, Ground-to-satellite quantum teleportation, *Nature* **549**, 70 (2017).
- [12] L. Geppert, Quantum transistors: toward nanoelectronics, *IEEE Spectr.* **37**, 46 (2000).
- [13] O. V. Marchukov, A. G. Volosniev, M. Valiente, D. Petrosyan, and N. Zinner, Quantum spin transistor with a heisenberg spin chain, *Nature communications* **7**, 1 (2016).
- [14] K. Joulain, J. Drevillon, Y. Ezzahri, and J. Ordonez-Miranda, Quantum thermal transistor, *Phys. Rev. Lett.* **116**, 200601 (2016).
- [15] N. J. S. Loft, L. B. Kristensen, C. K. Andersen, and N. T. Zinner, Quantum spin transistors in superconducting circuits, arXiv e-prints, arXiv:1802.04292 (2018), arXiv:1802.04292 [quant-ph].
- [16] M. A. de Ponte and A. C. Santos, Shortening time scale to reduce thermal effects in quantum transistors, *Sci. Rep.* **9**, 10470 (2019).
- [17] A. McRae, G. Wei, and A. Champagne, Graphene quantum strain transistors, *Phys. Rev. Appl.* **11**, 054019 (2019).
- [18] P. K. Shukla and B. Eliasson, Nonlinear theory for a quantum diode in a dense fermi magnetoplasma, *Phys. Rev. Lett.* **100**, 036801 (2008).
- [19] H. Shen, Y. Zhou, and X. Yi, Quantum optical diode with semiconductor microcavities, *Phys. Rev. A* **90**, 023849 (2014).
- [20] M. H. Devoret and C. Glattli, Single-electron transistors, *Phys. World* **11**, 29 (1998).
- [21] F. Arute, K. Arya, R. Babbush, D. Bacon, J. C. Bardin, R. Barends, R. Biswas, S. Boixo, F. G. S. L. Brandao, D. A. Buell, B. Burkett, Y. Chen, Z. Chen, B. Chiaro, R. Collins, W. Courtney, A. Dunsworth, E. Farhi, B. Foxen, A. Fowler, C. Gidney, M. Giustina, R. Graff, K. Guerin, S. Habegger, M. P. Harrigan, M. J. Hartmann, A. Ho, M. Hoffmann, T. Huang, T. S. Humble, S. V. Isakov, E. Jeffrey, Z. Jiang, D. Kafri, K. Kechedzhi, J. Kelly, P. V. Klimov, S. Knysh, A. Korotkov, F. Kostritsa, D. Landhuis, M. Lindmark, E. Lucero, D. Lyakh, S. Mandrà, J. R. McClean, M. McEwen, A. Megrant, X. Mi, K. Michielsen, M. Mohseni, J. Mutus, O. Naaman, M. Neale, C. Neill, M. Y. Niu, E. Ostby, A. Petukhov, J. C. Platt, C. Quintana, E. G. Rieffel, P. Roushan, N. C. Rubin, D. Sank, K. J. Satzinger, V. Smelyanskiy, K. J. Sung, M. D. Trevithick, A. Vainsencher, B. Villalonga, T. White, Z. J. Yao, P. Yeh, A. Zalcman, H. Neven, and J. M. Martinis, Quantum supremacy using a programmable superconducting processor, *Nature* **574**, 505 (2019).
- [22] D. Bacon and S. T. Flammia, Adiabatic gate teleportation, *Phys. Rev. Lett.* **103**, 120504 (2009).
- [23] A. C. Santos, R. D. Silva, and M. S. Sarandy, Shortcut to adiabatic gate teleportation, *Phys. Rev. A* **93**, 012311 (2016).
- [24] D. Gottesman and I. L. Chuang, Demonstrating the viability of universal quantum computation using teleportation and single-qubit operations, *Nature* **402**, 390 (1999).
- [25] H.-J. Briegel, W. Dür, J. I. Cirac, and P. Zoller, Quantum repeaters: The role of imperfect local operations in quantum communication, *Phys. Rev. Lett.* **81**, 5932 (1998).
- [26] D. P. DiVincenzo and D. Loss, Quantum computers and quantum coherence, *J. Magn. Mater.* **200**, 202 (1999).
- [27] F. Campaioli, F. A. Pollock, and S. Vinjanampathy, Quantum batteries, in *Thermodynamics in the Quantum Regime* (Springer, 2018) pp. 207–225.
- [28] S. Bhattacharjee and A. Dutta, Quantum thermal machines and batteries, *The European Physical Journal B* **94**, 1 (2021).
- [29] R. Alicki and M. Fannes, Entanglement boost for extractable work from ensembles of quantum batteries, *Phys. Rev. E* **87**, 042123 (2013).
- [30] A. C. Santos, B. Çakmak, S. Campbell, and N. T. Zinner, Stable adiabatic quantum batteries, *Phys. Rev. E* **100**, 032107 (2019).
- [31] G. M. Andolina, M. Keck, A. Mari, V. Giovannetti, and M. Polini, Quantum versus classical many-body batteries, *Phys. Rev. B* **99**, 205437 (2019).
- [32] V. Shaghaghghi, V. Singh, G. Benenti, and D. Rosa, Micromasers as quantum batteries, *Quantum Science and Technology* **7**, 04LT01 (2022).
- [33] C. A. Downing and T. J. Sturges, Directionality between driven-dissipative resonators, *Europhysics Letters* **140**, 35001 (2022).
- [34] G. M. Andolina, M. Keck, A. Mari, M. Campisi, V. Giovannetti, and M. Polini, Extractable work, the role of correlations, and asymptotic freedom in quantum batteries, *Phys. Rev. Lett.* **122**, 047702 (2019).
- [35] D. Farina, G. M. Andolina, A. Mari, M. Polini, and V. Giovannetti, Charger-mediated energy transfer for quantum batteries: An open-system approach, *Phys. Rev. B* **99**, 035421 (2019).
- [36] M. B. Arjmandi, A. Shokri, E. Faizi, and H. Mohammadi, Performance of quantum batteries with correlated and uncorrelated chargers, *Phys. Rev. A* **106**, 062609 (2022).



- [37] F. Campaioli, F. A. Pollock, F. C. Binder, L. Céleri, J. Goold, S. Vinjanampathy, and K. Modi, Enhancing the charging power of quantum batteries, *Phys. Rev. Lett.* **118**, 150601 (2017).
- [38] F. C. Binder, S. Vinjanampathy, K. Modi, and J. Goold, Quanta-cell: powerful charging of quantum batteries, *New J. Phys.* **17**, 075015 (2015).
- [39] D. Rossini, G. M. Andolina, D. Rosa, M. Carrega, and M. Polini, Quantum advantage in the charging process of sachdev-ye-kitaev batteries, *Phys. Rev. Lett.* **125**, 236402 (2020).
- [40] A. Crescente, M. Carrega, M. Sassetti, and D. Ferraro, Ultrafast charging in a two-photon dicke quantum battery, *Phys. Rev. B* **102**, 245407 (2020).
- [41] D. Ferraro, M. Campisi, G. M. Andolina, V. Pellegrini, and M. Polini, High-power collective charging of a solid-state quantum battery, *Phys. Rev. Lett.* **120**, 117702 (2018).
- [42] G. Francica, Quantum correlations and ergotropy, *Phys. Rev. E* **105**, L052101 (2022).
- [43] G. Francica, J. Goold, F. Plastina, and M. Paternostro, Dae-monic ergotropy: enhanced work extraction from quantum correlations, *npj Quantum Information* **1**, 12 (2017).
- [44] J. Q. Quach and W. J. Munro, Using dark states to charge and stabilize open quantum batteries, *Phys. Rev. Applied* **14**, 024092 (2020).
- [45] F. H. Kamin, F. T. Tabesh, S. Salimi, and A. C. Santos, Entanglement, coherence, and charging process of quantum batteries, *Phys. Rev. E* **102**, 052109 (2020).
- [46] S. Ghosh, T. Chanda, S. Mal, and A. Sen(De), Fast charging of a quantum battery assisted by noise, *Phys. Rev. A* **104**, 032207 (2021).
- [47] J. Monsel, M. Fellous-Asiani, B. Huard, and A. Auffèves, The energetic cost of work extraction, *Phys. Rev. Lett.* **124**, 130601 (2020).
- [48] G. Francica, F. C. Binder, G. Guarnieri, M. T. Mitchison, J. Goold, and F. Plastina, Quantum coherence and ergotropy, *Phys. Rev. Lett.* **125**, 180603 (2020).
- [49] A. C. Santos, Quantum advantage of two-level batteries in the self-discharging process, *Phys. Rev. E* **103**, 042118 (2021).
- [50] B. Çakmak, Ergotropy from coherences in an open quantum system, *Phys. Rev. E* **102**, 042111 (2020).
- [51] H.-L. Shi, S. Ding, Q.-K. Wan, X.-H. Wang, and W.-L. Yang, Entanglement, coherence, and extractable work in quantum batteries, *Physical Review Letters* **129**, 130602 (2022).
- [52] S. Tirone, R. Salvia, S. Chessa, and V. Giovannetti, Quantum work extraction efficiency for noisy quantum batteries: the role of coherence, *arXiv e-prints*, arXiv:2305.16803 (2023), arXiv:2305.16803 [quant-ph].
- [53] J.-Y. Gyhm, D. Šafránek, and D. Rosa, Quantum charging advantage cannot be extensive without global operations, *Physical Review Letters* **128**, 140501 (2022).
- [54] J. Joshi and T. S. Mahesh, Experimental investigation of a quantum battery using star-topology nmr spin systems, *Phys. Rev. A* **106**, 042601 (2022).
- [55] C.-K. Hu, J. Qiu, P. J. P. Souza, J. Yuan, Y. Zhou, L. Zhang, J. Chu, X. Pan, L. Hu, J. Li, Y. Xu, Y. Zhong, S. Liu, F. Yan, D. Tan, R. Bachelard, C. J. Villas-Boas, A. C. Santos, and D. Yu, Optimal charging of a superconducting quantum battery, *Quantum Science and Technology* **7**, 045018 (2022).
- [56] G. Gemme, M. Grossi, D. Ferraro, S. Vallecorsa, and M. Sassetti, Ibm quantum platforms: A quantum battery perspective, *Batteries* **8**, 10.3390/batteries8050043 (2022).
- [57] C. Cruz, M. F. Anka, M. S. Reis, R. Bachelard, and A. C. Santos, Quantum battery based on quantum discord at room temperature, *Quantum Sci. Technol.* **7**, 025020 (2022).
- [58] X. Huang, K. Wang, L. Xiao, L. Gao, H. Lin, and P. Xue, Demonstration of the charging progress of quantum batteries, *Phys. Rev. A* **107**, L030201 (2023).
- [59] J. L. da C Filho, Z. G. Izquierdo, A. Saguia, T. Albash, I. Hen, and M. S. Sarandy, Localization transition induced by programmable disorder, *Physical Review B* **105**, 134201 (2022).
- [60] J. A. Kjäll, J. H. Bardarson, and F. Pollmann, Many-body localization in a disordered quantum ising chain, *Physical review letters* **113**, 107204 (2014).
- [61] S. Ghosh, T. Chanda, A. Sen, *et al.*, Enhancement in the performance of a quantum battery by ordered and disordered interactions, *Phys. Rev. A* **101**, 032115 (2020).
- [62] D. Rossini, G. M. Andolina, and M. Polini, Many-body localized quantum batteries, *Phys. Rev. B* **100**, 115142 (2019).
- [63] A. E. Allahverdyan, R. Balian, and T. M. Nieuwenhuizen, Maximal work extraction from finite quantum systems, *Europhys. Lett.* **67**, 565 (2004).
- [64] L. F. C. Moraes, A. Saguia, A. C. Santos, and M. S. Sarandy, Charging power and stability of always-on transitionless driven quantum batteries, *Accepted for publication in EPL (Europhysics Letters)* (2021).
- [65] M. B. Arjmandi, H. Mohammadi, and A. C. Santos, Enhancing self-discharging process with disordered quantum batteries, *Phys. Rev. E* **105**, 054115 (2022).
- [66] I. Oliveira, R. Sarthour Jr, T. Bonagamba, E. Azevedo, and J. C. Freitas, *NMR quantum information processing* (Elsevier, Oxford, UK, 2011).
- [67] M. Žnidarič, T. Prosen, and P. Prelovšek, Many-body localization in the heisenberg  $x \times x \times z$  magnet in a random field, *Physical Review B* **77**, 064426 (2008).
- [68] A. Pal and D. A. Huse, Many-body localization phase transition, *Physical review b* **82**, 174411 (2010).
- [69] D. J. Luitz, N. Laflorencie, and F. Alet, Many-body localization edge in the random-field heisenberg chain, *Physical Review B* **91**, 081103 (2015).
- [70] K. V. Hovhannissyan, F. Barra, and A. Imparato, Charging assisted by thermalization, *Phys. Rev. Research* **2**, 033413 (2020).
- [71] Since by using a Jordan-Wigner transformation [87] the model can be mapped into a non-interacting fermionic model, for which any arbitrary degree of disorder is able to localize the system [60].
- [72] A. C. Santos, A. Saguia, and M. S. Sarandy, Stable and charge-switchable quantum batteries, *Phys. Rev. E* **101**, 062114 (2020).
- [73] R. Nandkishore and D. A. Huse, Many-body localization and thermalization in quantum statistical mechanics, *Annu. Rev. Condens. Matter Phys.* **6**, 15 (2015).
- [74] B. Krummheuer, V. M. Axt, and T. Kuhn, Theory of pure dephasing and the resulting absorption line shape in semiconductor quantum dots, *Physical Review B* **65**, 195313 (2002).
- [75] X. Fan, T. Takagahara, J. Cunningham, and H. Wang, Pure dephasing induced by exciton-phonon interactions in narrow gaas quantum wells, *Solid state communications* **108**, 857 (1998).
- [76] L. Besombes, K. Kheng, L. Marsal, and H. Mariette, Acoustic phonon broadening mechanism in single quantum dot emission, *Physical Review B* **63**, 155307 (2001).
- [77] A. Vagov, V. M. Axt, T. Kuhn, W. Langbein, P. Borri, and U. Woggon, Nonmonotonous temperature dependence of the initial decoherence in quantum dots, *Physical Review B* **70**, 201305 (2004).
- [78] Q. Turchette, C. Myatt, B. King, C. Sackett, D. Kielpinski, W. Itano, C. Monroe, and D. Wineland, Decoherence and decay of motional quantum states of a trapped atom coupled to engineered reservoirs, *Physical Review A* **62**, 053807 (2000).

- [79] C. J. Myatt, B. E. King, Q. A. Turchette, C. A. Sackett, D. Kielpinski, W. M. Itano, C. Monroe, and D. J. Wineland, Decoherence of quantum superpositions through coupling to engineered reservoirs, *Nature* **403**, 269 (2000).
- [80] A. C. Santos and M. S. Sarandy, Superadiabatic controlled evolutions and universal quantum computation, *Sci. Rep.* **5**, 15775 (2015).
- [81] I. B. Coulamy, A. C. Santos, I. Hen, and M. S. Sarandy, Energetic cost of superadiabatic quantum computation, *Frontiers in ICT* **3**, 19 (2016).
- [82] S. Campbell and S. Deffner, Trade-off between speed and cost in shortcuts to adiabaticity, *Phys. Rev. Lett.* **118**, 100601 (2017).
- [83] A. C. Santos and M. S. Sarandy, Generalized shortcuts to adiabaticity and enhanced robustness against decoherence, *J. Phys. A: Math. Theor.* **51**, 025301 (2018).
- [84] C.-K. Hu, J.-M. Cui, A. C. Santos, Y.-F. Huang, M. S. Sarandy, C.-F. Li, and G.-C. Guo, Experimental implementation of generalized transitionless quantum driving, *Opt. Lett.* **43**, 3136 (2018).
- [85] A. C. Santos, A. Nicotina, A. M. Souza, R. S. Sarthour, I. S. Oliveira, and M. S. Sarandy, Optimizing NMR quantum information processing via generalized transitionless quantum driving, *EPL (Europhysics Letters)* **129**, 30008 (2020).
- [86] S. Deffner, Energetic cost of hamiltonian quantum gates, *EPL (Europhysics Letters)* **134**, 40002 (2021).
- [87] S. Sachdev, Quantum phase transitions, *Physics world* **12**, 33 (1999).